

Article

# Improving the Electrochemical Performance of $\text{LiNi}_{0.80}\text{Co}_{0.15}\text{Al}_{0.05}\text{O}_2$ in Lithium Ion Batteries by $\text{LiAlO}_2$ Surface Modification

Chunhua Song , Wenge Wang, Huili Peng, Ying Wang \*, Chenglong Zhao \*, Huibin Zhang, Qiwei Tang, Jinzhao Lv, Xianjun Du and Yanmeng Dou

Shandong YuHuang New Energy Technology Co. Ltd., Heze 274000, China; ch.song@yhnewenergy.com (C.S.); wg.wang@yhnewenergy.com (W.W.); hl.peng@yhnewenergy.com (H.P.); hb.zhang@yhnewenergy.com (H.Z.); qw.tang@yhnewenergy.com (Q.T.); jz.lv@yhnewenergy.com (J.L.); xj.du@yhnewenergy.com (X.D.); ym.dou@yhnewenergy.com (Y.D.)

\* Correspondence: y.wang@yhnewenergy.com (Y.W.); cl.zhao@yhnewenergy.com (C.Z.)

Received: 27 October 2017; Accepted: 13 February 2018; Published: 5 March 2018

**Featured Application:**  $\text{LiNi}_{0.80}\text{Co}_{0.15}\text{Al}_{0.05}\text{O}_2$  can be used to fabricate high energy density lithium-ion batteries for uses including powering electric vehicles, energy storage (including communication base stations, wind power generation, solar power generation), and digital electronics.

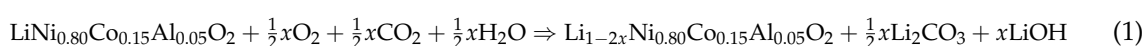
**Abstract:**  $\text{LiNi}_{0.80}\text{Co}_{0.15}\text{Al}_{0.05}\text{O}_2$  (NCA) as a lithium ion battery cathode material has received attention for its highly specific capacity and excellent low temperature performance. However, the disadvantages of its high surface lithium compound residues and high pH value have influenced its processing performance and limited its application. This paper uses a facile method to modify NCA through  $\text{LiAlO}_2$  coating. The results showed that when the molar ratio of  $\text{Al}(\text{NO}_3)_3 \cdot 9\text{H}_2\text{O}$  and lithium compound residues at the surface of NCA cathode material was 0.25:1, the pH of the cathode material decreased from 12.70 to 11.80 and the surface lithium compound residues decreased from 3.99% to 1.48%. The NCA cell was charged and discharged for 100 cycles at 1 C in the voltage range of 3.0–4.3 V, to test the capacity retention of NCA. It was found to be as high as 94.67%, which was 5.36% higher than the control NCA cell. The discharge capacity of NCA-0.25-500 °C was 139.8 mAh/g even at 8 C rate, which was 15% higher than the raw NCA. Further research indicated that  $\text{Al}(\text{NO}_3)_3 \cdot 9\text{H}_2\text{O}$  reacted with the surface lithium compound residues of NCA and generated  $\text{LiAlO}_2$ , which improved the NCA electrochemical performance.

**Keywords:**  $\text{LiNi}_{0.80}\text{Co}_{0.15}\text{Al}_{0.05}\text{O}_2$ ;  $\text{LiAlO}_2$  coating; lithium compound residues; pH value; capacity retention

## 1. Introduction

Lithium ion batteries (LIBs) are the next generation of power sources for technology such as electric vehicles, mobile phones, and notebook computers, due to its higher energy density, longer cyclic life, faster charge/discharge rates, and better safety. The performance of cathode materials is one of the most important factors that determine the performance of a battery. Therefore, developing a cathode material with high energy density, long cyclic life, and high security is essential [1]. Nickel-rich cathode material  $\text{Li}(\text{Ni}_x\text{M}_{1-x})\text{O}_2$  is one of the most applicable cathode materials for advanced LIBs, due to its high energy, power density, and lower cost [2]. Intense research efforts have found that Co and Al co-doping could stabilise the layered structure of  $\text{LiNiO}_2$ . To date, a Co and Al co-doped NCA has been successfully designed, and it shows excellent thermodynamic stability and electrochemical reactivity with a specific capacity as high as 200 mAh/g. Therefore, NCA shows promise as a candidate for lithium ion batteries, particularly for use in electric vehicles.

However, some aspects of NCA remain problematic such as poor cycle stability, low electronic conductivity, and the disordered spinel structure in the charged states due to its inherent shortcomings with instability structure at elevated voltages [3–5]. NCA has been synthesized by various methods including Co-precipitation which is the most common method. To compensate for the loss of lithium at high temperature, excessive lithium is needed in the preparation, however it does not completely evaporate during the high temperature solid phase reaction. Some lithium oxide (Li<sub>2</sub>O) remains on the surface of the cathode materials which can react directly with CO<sub>2</sub> and atmospheric H<sub>2</sub>O to generate Li<sub>2</sub>CO<sub>3</sub> and LiOH [6], as in the reaction shown at Equation (1). In the coating process of battery fabrication, the slurry readily forms a gel and loses its binding ability, which is detrimental to the foil coating. Furthermore, Li<sub>2</sub>CO<sub>3</sub> may react with HF and generate CO<sub>2</sub>, resulting in high temperature inflatable and cyclic performance degradation [4]. Additionally, under the highly delithiated state, the reduction of Ni<sup>4+</sup> to Ni<sup>2+</sup> occurred on the NCA surface and led to the release of O<sub>2</sub>, and the consequent thermal instability and safety problems.



To reduce the residual lithium compound and the pH of NCA, intensive methods have been developed recently:

- (i.) Controlling the residual lithium compound content by reducing the proportion of lithium salt or by extending the time of the solid phase reaction at high temperature.
- (ii.) Washing the cathode materials several times in water, carbonate, organic acids, or organic solvents.
- (iii.) Enhancing the capacity and electronic conductivity by coating the electroactive materials; TiO<sub>2</sub>, AlF<sub>3</sub>, Al<sub>2</sub>O<sub>3</sub>, SiO<sub>2</sub>, and AlPO<sub>4</sub> have been suggested as suitable coating materials for the layered cathodes [7–16]. The coating material mainly acts as an isolation layer to prevent side reactions and reduce the pH, which improved thermal stability and cycling stability of the cathode materials.

In this study, we improved the performance of Ni-rich cathode material NCA using a facile method by modifying LiAlO<sub>2</sub>. The results revealed that the residual lithium compound and the pH of NCA was successfully reduced by coating it with LiAlO<sub>2</sub>. Furthermore, the SEM images of NCA indicated that the layer was distributed uniformly on the cathode material, which could enhance process ability, safety, and the electrochemical performance of lithium ion batteries.

## 2. Experiment

### 2.1. Synthesis of NCA

All reagents were purchased from Sinopharm Chemical Reagent Co., Ltd. (Shanghai, China). All chemicals were used without further purification. NiSO<sub>4</sub>·6H<sub>2</sub>O, CoSO<sub>4</sub>·7H<sub>2</sub>O, and Al<sub>2</sub>(SO<sub>4</sub>)<sub>3</sub>·18H<sub>2</sub>O were mixed at a molar ratio of Ni<sup>2+</sup>:Co<sup>2+</sup>:Al<sup>3+</sup> = 80:15:5. This mixed solution was pumped slowly into a continuously stirred tank reactor. At same time, a NaOH and NH<sub>4</sub>OH composite solution was also pumped into the reactor and the pH value controlled at 11.4. After the reaction, the precipitate was filtered and washed with distilled water to remove the residual ions. The precipitation was then dried in a vacuum oven at 120 °C for 12 h to obtain the (Ni<sub>0.80</sub>Co<sub>0.15</sub>Al<sub>0.05</sub>)(OH)<sub>2</sub> precursor.

The (Ni<sub>0.80</sub>Co<sub>0.15</sub>Al<sub>0.05</sub>)(OH)<sub>2</sub> precursor and LiOH·H<sub>2</sub>O were mixed thoroughly with LiOH·H<sub>2</sub>O 5% excess in a molar ratio. The mixture was heated at 450 °C for 6 h, then calcined at 780 °C for 12 h in oxygen at a heating rate of 2 °C/min. NCA was prepared after crushing and sieving.

## 2.2. LiAlO<sub>2</sub> Modified NCA

The cathode material obtained was mixed thoroughly with Al(NO<sub>3</sub>)<sub>3</sub>·9H<sub>2</sub>O by milling in an agate mortar for 30 min. The mixture was first handled at 75 °C for 2 h in air, and then calcined at different temperatures for 2 h with a heating rate of 5 °C/min. NCA with the molar ratio of Al(NO<sub>3</sub>)<sub>3</sub> and residual Li<sub>2</sub>CO<sub>3</sub> of the cathode surface being 0.25 were calcined at 400 °C, 500 °C and 600 °C for 2 h, which are expressed as NCA-0.25-400 °C, NCA-0.25-500 °C and NCA-0.25-600 °C, respectively. Products calcined at 500 °C for 2 h are labeled as NCA-2, NCA-0.5 and NCA-0.25 with the molar ratio of Al(NO<sub>3</sub>)<sub>3</sub> and excess Li<sub>2</sub>CO<sub>3</sub> at the surface of NCA being 2, 0.5 and 0.25, respectively.

## 2.3. Material Characterizations

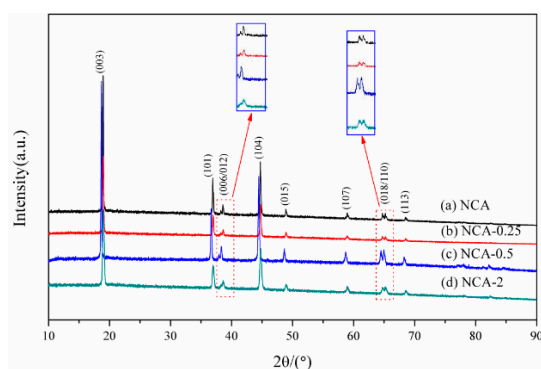
The phase of all samples were identified by X-ray diffraction (XRD, D2 Phaser, Bruker, Karlsruhe, Germany) using Cu K $\alpha$  radiation at 40 kV and 40 mA. The scanning range of the diffraction angle (2 $\theta$ ) was 10–90°. The morphologies of products were determined by scanning electron microscope (Ultra plus, Zeiss, Oberkochen, Germany). The electrochemical impedance spectroscopy (EIS) measures were performed using an impedance analyzer (CHI660E, CH, Shanghai, China) over the frequency range of 0.002–1000 Hz with AC voltage amplitude of 5 mV.

## 2.4. Electrochemical Measurement

CR2032 coin-type cells were used for the electrochemical test. The cathode electrode consisted of 88 wt % active material, 3 wt % acetylene black (Super P), 3 wt % conductive graphite (ks-6) and 6 wt % PVDF binder. A lithium metal foil was used as the anode. A polypropylene film (Cellgard 2400) was used as the separator. LiPF<sub>6</sub> in a 1:1:1 (v/v/v) mixture of ethylene carbonate (EC), dimethyl carbonate (DMC), and ethyl methyl carbonate (EMC) was used as the electrolyte. Assembly of the cells was carried out in a dry Ar-filled glove box (UNILab, MBRAUN, Garching, Germany). Galvanostatic charge-discharge tests were performed at a voltage range of 3.0–4.3 V on a battery testing system (CT2001A, LANHE, Wuhan, China).

## 3. Results and Discussion

Figure 1 shows the XRD diffraction profiles of the NCA with different coating contents of LiAlO<sub>2</sub>. As can be seen, the diffraction patterns of all samples are well-indexed to the hexagonal  $\alpha$ -NaFeO<sub>2</sub> structure with a space group  $R\bar{3}m$ . All samples display clear diffraction peaks without any discernable secondary phase. The clear splitting of (006)/(012) and (018)/(110) peak pairs for NCA, NCA-0.25 and NCA-0.5 suggests the formation of highly ordered hexagonal layered structure [1,17]. The results suggest that the crystal structure of NCA is not affected by a small amount of LiAlO<sub>2</sub>. As seen in the diffraction patterns of NCA-2, the separation of (006)/(012) and (018)/(110) peak pairs is not clear, indicating that increasing amounts of Al(NO<sub>3</sub>)<sub>3</sub>·9H<sub>2</sub>O will influence the crystalline structure of NCA.



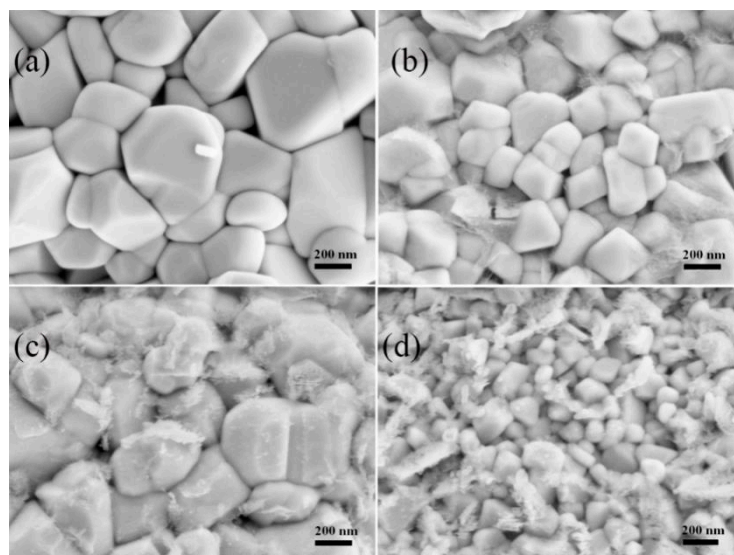
**Figure 1.** XRD patterns of four samples, NCA, NCA-0.25, NCA-0.5 and NCA-2.

Table 1 presents the values of  $a$ ,  $c$ ,  $c/a$ ,  $I_{003}/I_{104}$  calculated from XRD patterns of the samples. The ionic radius of  $\text{Ni}^{2+}$  ( $r = 70$  pm) is close to  $\text{Li}^+$  ( $r = 74$  pm), which results in the migration of some of the  $\text{Ni}^{2+}$  ions to  $\text{Li}^+$  sites. The extent of cation mixing is usually evaluated by the intensity ratio of (003)/(104). Higher values of  $I_{003}/I_{104}$  correspond to a low extent of cation mixing. It can be seen from Table 1 that the value of  $I_{003}/I_{104}$  of all samples are higher than 1.2, which indicates that the samples have a low degree of cation mixing [17]. It is noted that the lattice parameter increases with the addition of  $\text{Al}(\text{NO}_3)_3 \cdot 9\text{H}_2\text{O}$ , but the value of  $c/a$  is not reduced. Larger ratios of  $c/a$  bring greater degrees of crystallinity and stability of the NCA with layered structure [18].

**Table 1.** Lattice parameters and the values of  $I_{003}/I_{104}$  for NCA, NCA-0.25, NCA-0.5 and NCA-2.

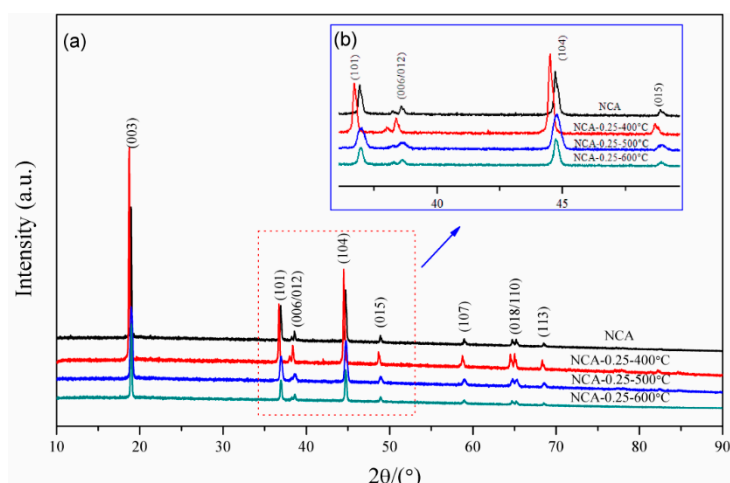
Sample	$a$ ( $\pm 0.0003$ Å)	$c$ ( $\pm 0.0004$ Å)	$c/a$	$I_{003}/I_{104}$
NCA	2.8576	14.0508	4.92	2.35
NCA-0.25	2.8601	14.0340	4.91	2.19
NCA-0.5	2.8677	14.2335	4.96	1.90
NCA-2	2.8648	14.0131	4.89	2.31

The SEM images of NCA, NCA-0.25, NCA-0.5, and NCA-2 are shown in Figure 2 and it can be seen that the surface of the pristine NCA is smooth. After  $\text{LiAlO}_2$  modification, a layer appears on the surface of NCA and the surface becomes rough, which increases with increasing amount of  $\text{Al}(\text{NO}_3)_3$  [1,18]. From Figure 2b, it can be seen that there are some floccules on the particle surface and between the particle clearances. When the molar ratio of  $\text{Al}(\text{NO}_3)_3 \cdot 9\text{H}_2\text{O}$  and residual  $\text{Li}_2\text{CO}_3$  of the NCA surface is 0.5:1, more floccules are present between the particles and some floccules are agglomerated. Even at the molar ratio of  $\text{Al}(\text{NO}_3)_3 \cdot 9\text{H}_2\text{O}$  and residual  $\text{Li}_2\text{CO}_3$  is 2:1, the agglomerated floccules appear on the surface of NCA. In combination with the XRD, the layered structure of NCA is optimal at a molar ratio of  $\text{Al}(\text{NO}_3)_3 \cdot 9\text{H}_2\text{O}$  and residual  $\text{Li}_2\text{CO}_3$  of 0.25.



**Figure 2.** SEM images of the as-prepared samples (a) NCA, (b) NCA-0.25, (c) NCA-0.5, (d) NCA-2.

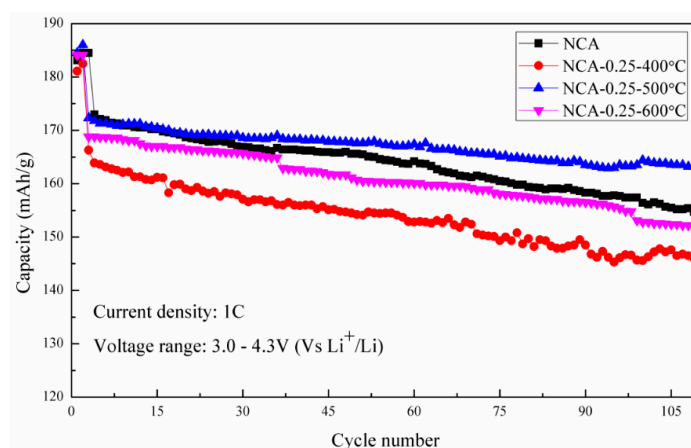
Figure 3 displays the XRD patterns of NCA-0.25 under different calcination temperatures. The diffraction patterns of samples correspond to the hexagonal  $\alpha\text{-NaFeO}_2$  structure with a space group  $R\bar{3}m$ . When the calcination temperature is 400 °C (Figure 3b), the position of all peaks shifts slightly toward the lower degree. At the calcination temperature of 500 °C and 600 °C, there are no peaks of the impurity phase, indicating that the structure of the sample is not destroyed.



**Figure 3.** (a) XRD patterns of the pristine NCA sample and NCA-0.25 samples at different calcination temperature from 400 °C to 600 °C, and (b) the magnified patterns of (a) between 33° and 50°.

NCA with higher pH values reacts readily with  $\text{CO}_2$  and atmospheric  $\text{H}_2\text{O}$  and results in a degraded electrochemical performance. Therefore, unmodified NCA is detrimental to long term storage. Figure 4 shows the cycle performance of the pristine NCA sample and the NCA-0.25 samples at different calcination temperatures from 400 °C to 600 °C. Table 2 shows that when the molar ratio of  $\text{Al}(\text{NO}_3)_3 \cdot 9\text{H}_2\text{O}$  and residual  $\text{Li}_2\text{CO}_3$  of the NCA surface is 0.25, the pH value and residual alkaline of materials is reduced, which is beneficial to storage performance.  $\text{LiAlO}_2$  modified NCA shows no improvements in first discharge capacity.

However, the discharge capacity of  $\text{LiAlO}_2$  modified NCA is significantly higher than the raw materials at 1 C rate. Furthermore, capacity retention of  $\text{LiAlO}_2$  modified NCA is higher than the raw materials. The results indicate that  $\text{LiAlO}_2$  modification can improve the electrochemical properties and physical properties of the cathode materials. The NCA-0.25-400 °C exhibits an initial discharge capacity of 166.3 mAh/g at 1 C and capacity retention of 88.03% after 100 cycles. When the calcination temperature of NCA-0.25 is 500 °C and 600 °C, the initial discharge capacity is 172.3 and 168.6 mAh/g at 1 C, and its capacity retention is 94.67% and 92.88%, respectively. Based on XRD analysis, the optimum electrochemical performance is when the calcination temperature of NCA-0.25 is 500 °C. At the same time, in order to avoid the uncertainty of the data caused by the accident of one measurement, we take the average value of each parallel test three times, the results are appropriate, seeing Table S1 and Figure S1.

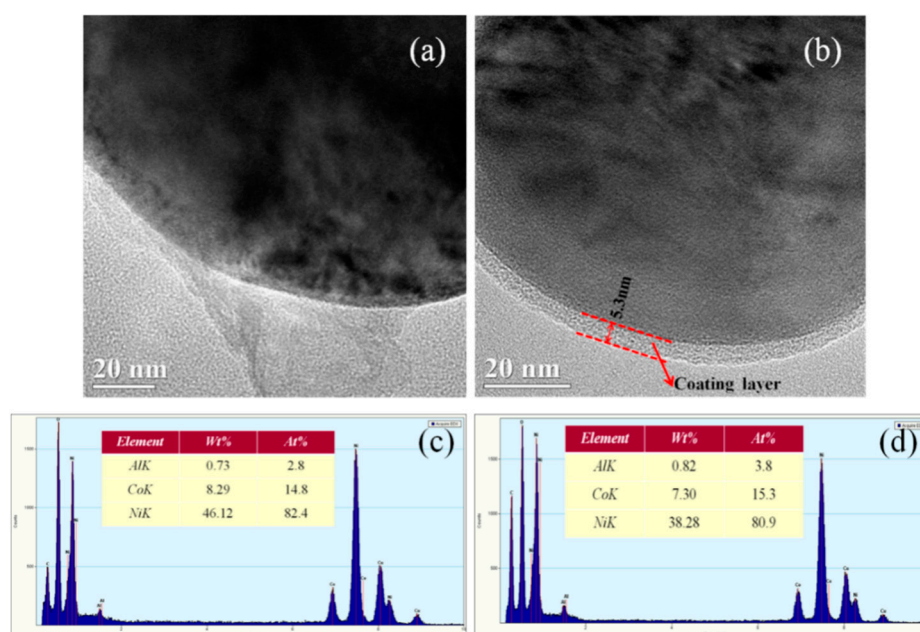


**Figure 4.** Cyclic performance of the pristine NCA sample and NCA-0.25 samples at different calcination temperatures from 400 °C to 600 °C.

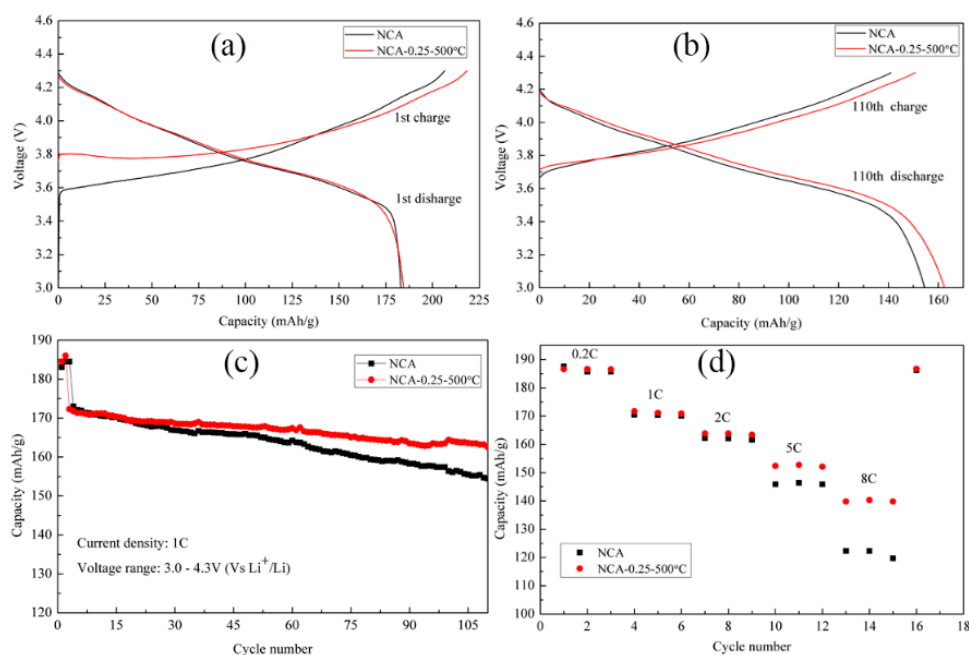
**Table 2.** Physical and chemical properties of the pristine NCA sample and NCA-0.25 samples at different calcination temperatures from 400 °C to 600 °C.

Sample	pH	Residual Alkaline (Li <sub>2</sub> CO <sub>3</sub> % + LiOH%)	First Discharge Capacity at 0.2 C (mAh/g)	First Discharge Efficiency (%)	Discharge Capacity at 1 C (mAh/g)	110 Cycles Capacity Retention (%)
NCA	12.70	3.99%	183.1	88.6%	173.0	89.31%
NCA-0.25-400 °C	11.86	1.78%	181.1	83.1%	166.3	88.03%
NCA-0.25-500 °C	11.80	1.48%	184.5	83.8%	172.3	94.67%
NCA-0.25-600 °C	11.82	1.38%	184.1	84.3%	168.6	92.88%

The TEM and EDS images of pristine NCA and NCA-0.25 are shown in Figure 5. The TEM images show that there is a significant difference in the particle surface before and after coating with a uniform coating layer of about 5.3 nm after LiAlO<sub>2</sub> modification (Figure 5b). The results indicate that the Al(NO<sub>3</sub>)<sub>3</sub>·9H<sub>2</sub>O reacted with the surface lithium compound residues and generated LiAlO<sub>2</sub>, which can suppress the reactions between the electrode and the electrolyte, and facilitated the charge transfer process. The composition of NCA was examined by EDS, and it was found that NCA had typical diffraction peaks of O, Ni, Co, Al. The molar ratio of Ni, Co and Al was 82.4:14.8:2.8, which is close to the NCA molecular formula. Because Al(OH)<sub>3</sub> is a bisexual compound, it is difficult to co-precipitate Al with Ni and Co, and the actual Al content is smaller than 5%. Furthermore, the content of aluminum on the particle surface of NCA increased to 3.8% after LiAlO<sub>2</sub> modification [11].

**Figure 5.** TEM micrographs of the pristine NCA (a) and NCA-0.25 (b), EDS pattern of the pristine NCA (c) and NCA-0.25 (d).

Electrochemical measurements were taken to investigate the influence of LiAlO<sub>2</sub> on the electrochemical performances of NCA. Figure 6a shows the initial charge/discharge curves of NCA and NCA-0.25-500 °C at 0.2 C. The initial coulombic efficiencies of NCA and NCA-0.25-500 °C are 88.6% and 83.8%, respectively. Despite the initial coulombic efficiencies, they declined after LiAlO<sub>2</sub> modification, however the difference is small. When cells were cycled for 100 cycles at 1 C, the discharge capacities of raw NCA and NCA-0.25-500 °C were 154.5 and 163.1 mAh/g (Figure 6b), respectively, indicating that LiAlO<sub>2</sub> can improve the cycling stability of NCA [19].



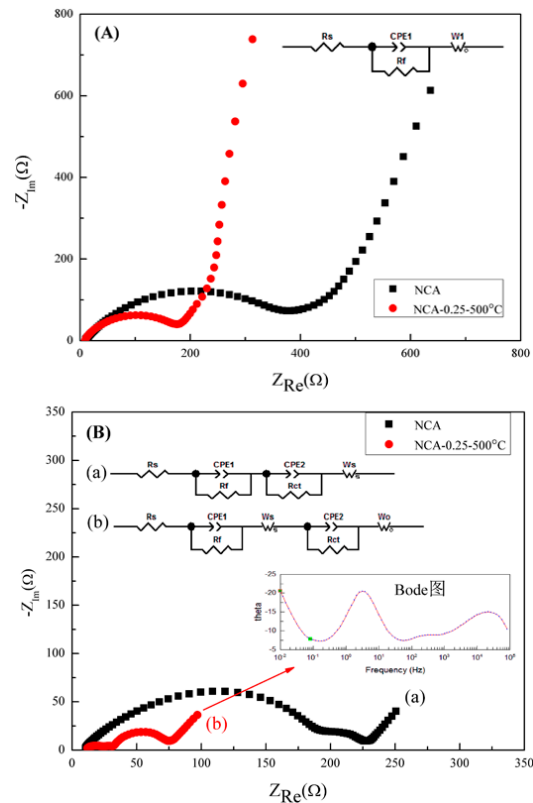
**Figure 6.** Charge and discharge profiles at the first cycle at 0.2 C (a) and at the 110th cycle at 1 C (b) of the as-prepared samples; the cycle performances at 1 C (c) and rate capability (d) of the as-prepared samples.

Figure 6c shows the cycling performances for 100 cycles at 1C in the voltage range of 3.0–4.3 V and it shows that NCA exhibits a rapid discharge capacity fading after 100 cycles and a low capacity retention of 89.31%. The lower capacity retention suggests that electrode materials may react with electrolyte and generate particles on the surface, which hinder the lithium ions intercalation. In contrast, NCA-0.25-500 °C shows a better cyclic performance with a lower discharge fading after 100 cycles and a relatively high capacity retention of 94.67%. This indicates that  $\text{LiAlO}_2$  modification can restrain the capacity degradation effectively. To examine the rate capabilities of raw NCA and NCA-0.25-500 °C, discharge capabilities were taken at 0.2 C, 1 C, 2 C, 5 C and 8 C. As shown in Figure 6d, compared to NCA, NCA-0.25-500 °C show better discharge capacity and cycle stability as the discharge rate increased. This is especially so when the discharge capacities of NCA-0.25-500 °C is 139.8 mAh/g at 8 C rate, which is 15% higher than NCA. This is mainly due to the more stable structure during cycling of NCA with the coating layer, which can protect the particle from the side reactions on the surface. Therefore,  $\text{LiAlO}_2$  modification can improve the discharge capacities and cyclic stability.

The electrochemical impedance spectra (EIS) of the samples are shown in Figure 7. Figure 7a shows electrochemical impedance spectroscopy and equivalent circuit of samples before discharge [20]. Figure 7b shows electrochemical impedance spectroscopy and equivalent circuit of samples after 25 charge–discharge cycles at 1 C. The circuit elements of  $R_s$ ,  $R_f$ ,  $R_{ct}$ , CPE,  $W_s$  and  $W_o$  represent the internal resistance of the cell, the surface film resistance (the resistance of SEI film), the charge-transfer resistance, constant phase element, the  $\text{Li}^+$  diffusion in finite thin layer impedance, and the Warburg electrode bulk, respectively [21].

As can be seen from Figure 7a, the assembled cell displays a single semicircle at the higher frequency and a straight line at low frequency, which corresponds to the surface film resistance and Warburg resistance. It can be seen from Figure 7a that there is no charge-transfer resistance due to the fact that the anode has no electrochemical reaction before charge-discharge [22]. Table 3 shows the impedances of  $\text{LiAlO}_2$  modified samples drastically decreased compared to the raw material. This phenomenon illustrates that  $\text{LiAlO}_2$  modification is beneficial to charge migration on the electrode interface and could decrease the battery internal impedance.

After 25 cycles, it can be seen that in EIS the charge-transfer resistance is formed. The EIS spectra of raw material consists of two semicircles and a line. The EIS spectra of  $\text{Al}(\text{NO}_3)_3 \cdot 9\text{H}_2\text{O}$  modified samples consist of three semicircles and a line. The second semicircle is well-known to have originated from the surface layer resistance, which is ascribed to the formation of a film on the particle surface after  $\text{LiAlO}_2$  modification. Table 3 shows the electrode resistance increases after  $\text{LiAlO}_2$  modification, at the same time, it can protect the cathode material from contacting the electrolyte. Moreover, finite thin layer impedance and the charge-transfer resistance of  $\text{LiAlO}_2$  modified samples were lower than that of the raw material, indicating that  $\text{LiAlO}_2$  can improve the electrochemical performance of NCA.



**Figure 7.** Electrochemical impedance spectra (EIS) of the lithium ion cells assembled with different electrodes, which were obtained before discharge (a) and after 25 cycles at 1 C rate (b). All impedance data were obtained at 4.3 V.

**Table 3.** Independent resistive components of the pristine NCA sample and NCA-0.25 samples analysed using an equivalent circuit.

Sample	Original			After 25 Cycles				
	Rs	Rf	Wo	Rs	Rct	Rf	Ws	Wo
NCA	8.28	327.01	372.60	9.16	200.20	13.62	160.90	—
NCA-0.25	8.71	159.70	82.43	9.93	9.54	32.06	11.57	29.65

#### 4. Conclusions

NCA has been successfully prepared by the co-precipitation method. After  $\text{LiAlO}_2$  modification, the surface lithium compound residues and pH of the cathode material was reduced. When the molar ratio of  $\text{Al}(\text{NO}_3)_3 \cdot 9\text{H}_2\text{O}$  and residual  $\text{Li}_2\text{CO}_3$  of the NCA surface is 0.25:1, the pH is 11.80 and the surface lithium residue is 1.48%, which could improve its processing performance. Although the initial discharge specific capacity slightly decreased after  $\text{LiAlO}_2$  modification, the high-rate ability

and the cycling stability improved. Furthermore, the impedances of cathode material decreased and the reversibility of lithium emergence/insertion increased after  $\text{LiAlO}_2$  coating. Therefore,  $\text{LiAlO}_2$  modification could improve NCA electrochemical performance. The capacity retention increased from 89.31% to 94.67% at 1 C between 3.0 and 4.3 V at 1 C after 100 cycles.

**Supplementary Materials:** The following are available online at [www.mdpi.com/2076-3417/8/3/378/s1](http://www.mdpi.com/2076-3417/8/3/378/s1), Figure S1: The mean and standard deviation diagrams of the three discharge of NCA series (NCA, NCA-0.25-400 °C, NCA-0.25-500 °C and NCA-0.25-600 °C): blue, green and grey histograms correspond to discharge at 0.2 C, discharge at 1 C and discharge at 1 C after 110 cycles, respectively., Table S1: The each, mean and standard deviation of the three discharge of NCA, NCA-0.25-400 °C, NCA-0.25-500 °C and NCA-0.25-600 °C, respectively.

**Acknowledgments:** We gratefully acknowledge financial supports from the Department of Science and Technology of Shandong Province (2017CXGC0503, 2016PT07), Shan Dong Economic and Information Technology Committee(201731917004).

**Author Contributions:** Chunhua Song, Ying Wang and Chenglong Zhao conceived and designed the experiments; Wenge Wang, Huibin Zhang and Qiwei Tang performed the experiments; Chunhua Song, Ying Wang, Chenglong Zhao and Wenge Wang analyzed the data; Jinzhao Lv, Xianjun Du and Yanmeng Dou contributed reagents/materials/analysis tools; Chunhua Song, Wenge Wang and Huili Peng wrote the paper.

**Conflicts of Interest:** The authors declare no conflict of interest.

## References

1. Zhou, P.; Zhang, Z.; Meng, H.; Lu, Y.; Cao, J.; Cheng, F.; Tao, Z.; Chen, J.  $\text{SiO}_2$ -coated  $\text{LiNi}_{0.915}\text{Co}_{0.075}\text{Al}_{0.01}\text{O}_2$  cathode material for rechargeable Li-ion batteries. *Nanoscale* **2016**, *8*, 19263–19269. [[CrossRef](#)] [[PubMed](#)]
2. Xu, Y.; Li, X.; Wang, Z.; Guo, H.; Huang, B. Structure and electrochemical performance of  $\text{TiO}_2$ -coated  $\text{LiNi}_{0.80}\text{Co}_{0.15}\text{Al}_{0.05}\text{O}_2$  cathode material. *Mater. Lett.* **2015**, *143*, 151–154. [[CrossRef](#)]
3. Ruan, Z.; Zhu, Y.; Teng, X. Effect of pre-thermal treatment on the lithium storage performance of  $\text{LiNi}_{0.8}\text{Co}_{0.15}\text{Al}_{0.05}\text{O}_2$ . *J. Mater. Sci.* **2016**, *51*, 1400–1408. [[CrossRef](#)]
4. Kleiner, K.; Melke, J.; Merz, M.; Jakes, P.; Nagel, P.; Schuppler, S.; Liebau, V.; Ehrenberg, H. Unraveling the Degradation Process of  $\text{LiNi}_{0.8}\text{Co}_{0.15}\text{Al}_{0.05}\text{O}_2$  Electrodes in Commercial Lithium Ion Batteries by Electronic Structure Investigations. *ACS Appl. Mater. Interfaces* **2015**, *7*, 19589–19600. [[CrossRef](#)] [[PubMed](#)]
5. Watanabe, S.; Kinoshita, M.; Hosokawa, T.; Morigaki, K.; Nakura, K. Capacity fade of  $\text{LiAl}_y\text{Ni}_{1-x-y}\text{Co}_x\text{O}_2$  cathode for lithium-ion batteries during accelerated calendar and cycle life tests (surface analysis of  $\text{LiAl}_y\text{Ni}_{1-x-y}\text{Co}_x\text{O}_2$  cathode after cycle tests in restricted depth of discharge ranges). *J. Power Sources* **2014**, *258*, 210–217. [[CrossRef](#)]
6. Yoon, S.H.; Lee, C.W.; Bae, Y.S.; Hwang, I.Y.; Park, Y.K.; Song, J.H. Method of Preparation for Particle Growth Enhancement of  $\text{LiNi}_{0.8}\text{Co}_{0.15}\text{Al}_{0.05}\text{O}_2$ . *Electrochem. Solid-State Lett.* **2009**, *12*, A211–A214. [[CrossRef](#)]
7. Dai, G.; Yu, M.; Shen, F.; Cao, J.; Ni, L.; Chen, Y.; Tang, Y. Improved cycling performance of  $\text{LiNi}_{0.8}\text{Co}_{0.15}\text{Al}_{0.05}\text{O}_2/\text{Al}_2\text{O}_3$  with core-shell structure synthesized by a heterogeneous nucleation-and-growth process. *Ionics* **2016**, *22*, 2021–2026. [[CrossRef](#)]
8. Nurpeissova, A.; Choi, M.H.; Kim, J.S.; Myung, S.K.; Kim, S.S.; Sun, Y.K. Effect of titanium addition as nickel oxide formation inhibitor in nickel-rich cathode material for lithium-ion batteries. *J. Power Sources* **2015**, *299*, 425–433. [[CrossRef](#)]
9. Zhang, L.; Luo, F.; Wang, J.; Guo, Y. Surface Coating and Electrochemical Properties of  $\text{LiNi}_{0.8}\text{Co}_{0.15}\text{Al}_{0.05}\text{O}_2$  Cathode in Lithium-Ion Cells. *Adv. Mater. Res.* **2014**, *1058*, 317–320. [[CrossRef](#)]
10. Zhu, L.; Liu, Y.; Wu, W.; Wu, X.; Tang, W.; Wu, Y. Surface fluorinated  $\text{LiNi}_{0.8}\text{Co}_{0.15}\text{Al}_{0.05}\text{O}_2$  as a positive electrode material for lithium ion batteries. *J. Mater. Chem. A* **2015**, *3*, 15156–15162. [[CrossRef](#)]
11. Li, X.; Xie, Z.; Liu, W.; Ge, W.; Wang, H.; Qu, M. Effects of fluorine doping on structure, surface chemistry, and electrochemical performance of  $\text{LiNi}_{0.8}\text{Co}_{0.15}\text{Al}_{0.05}\text{O}_2$ . *Electrochim. Acta* **2015**, *174*, 1122–1130. [[CrossRef](#)]
12. Li, L.; Chen, Z.; Zhang, Q.; Xu, M.; Zhou, X.; Zhu, H.; Zhang, K. A hydrolysis-hydrothermal route for the synthesis of ultrathin  $\text{LiAlO}_2$ -inlaid  $\text{LiNi}_{0.5}\text{Co}_{0.2}\text{Mn}_{0.3}\text{O}_2$  as a high-performance cathode material for lithium ion batteries. *J. Mater. Chem. A* **2015**, *3*, 894–904. [[CrossRef](#)]
13. Qin, C.; Cao, J.; Chen, J.; Dai, G.; Wu, T.; Chen, Y.; Tang, Y.; Li, A.; Chen, Y. Improvement of electrochemical performance of nickel rich  $\text{LiNi}_{0.6}\text{Co}_{0.2}\text{Mn}_{0.2}\text{O}_2$  cathode active material by ultrathin  $\text{TiO}_2$  coating. *Dalton Trans.* **2016**, *45*, 9669–9675. [[CrossRef](#)] [[PubMed](#)]

14. Lee, M.J.; Noh, M.; Park, M.H.; Jo, M.; Kim, H.; Nam, H.; Cho, J. The role of nanoscale-range vanadium treatment in  $\text{LiNi}_{0.8}\text{Co}_{0.15}\text{Al}_{0.05}\text{O}_2$  cathode materials for Li-ion batteries at elevated temperatures. *J. Mater. Chem. A* **2015**, *3*, 13453–13460. [[CrossRef](#)]
15. Tran, H.Y.; Täubert, C.; Fleischhammer, M.; Axmann, P.; Küppers, L.; Wohlfahrt-Mehrens, M.  $\text{LiMn}_2\text{O}_4$  Spinel/ $\text{LiNi}_{0.8}\text{Co}_{0.15}\text{Al}_{0.05}\text{O}_2$  Blends as Cathode Materials for Lithium-Ion Batteries. *J. Electrochem. Soc.* **2011**, *158*, A556–A561. [[CrossRef](#)]
16. Cho, Y.; Cho, J. Significant Improvement of  $\text{LiNi}_{0.8}\text{Co}_{0.15}\text{Al}_{0.05}\text{O}_2$  Cathodes at 60 °C by  $\text{SiO}_2$  Dry Coating for Li-Ion Batteries. *J. Electrochem. Soc.* **2010**, *157*, A625–A629. [[CrossRef](#)]
17. Chen, Y.; Li, P.; Zhao, S.; Zhuang, Y.; Zhao, S.; Zhou, Q.; Zheng, J. Influence of integrated microstructure on the performance of  $\text{LiNi}_{0.8}\text{Co}_{0.15}\text{Al}_{0.05}\text{O}_2$  as a cathodic material for lithium ion batteries. *RSC Adv.* **2017**, *7*, 29233–29239. [[CrossRef](#)]
18. Wu, F.; Wang, M.; Su, W.; Chen, S.; Xu, B. Effect of  $\text{TiO}_2$ -coating on the electrochemical performances of  $\text{LiCo}_{1/3}\text{Ni}_{1/3}\text{Mn}_{1/3}\text{O}_2$ . *J. Power Sources* **2009**, *191*, 628–632. [[CrossRef](#)]
19. Lee, D.J.; Scrosati, B.; Sun, Y.K.  $\text{Ni}_3(\text{PO}_4)_2$ -coated  $\text{Li}[\text{Ni}_{0.8}\text{Co}_{0.15}\text{Al}_{0.05}]\text{O}_2$  lithium battery electrode with improved cycling performance at 55 °C. *J. Power Sources* **2011**, *196*, 7742–7746. [[CrossRef](#)]
20. Aurbach, D.; Levi, M.D.; Levi, E.; Teller, H.; Markovsky, B.; Salitra, G.; Heider, U.; Heider, L. Common Electroanalytical Behavior of Li Intercalation Processes into Graphite and Transition Metal Oxides. *J. Electrochem. Soc.* **1988**, *145*, 3024–3034. [[CrossRef](#)]
21. Bai, Y.; Wang, X.; Zhang, X.; Shu, H.; Yang, X.; Hu, B.; Wei, Q.; Wu, H.; Song, Y. The kinetics of Li-ion deintercalation in the Li-rich layered  $\text{Li}_{1.12}[\text{Ni}_{0.5}\text{Co}_{0.2}\text{Mn}_{0.3}]_{0.89}\text{O}_2$  studied by electrochemical impedance spectroscopy and galvanostatic intermittent titration technique. *Electrochim. Acta* **2013**, *109*, 355–364. [[CrossRef](#)]
22. Liu, T.; Garsuch, A.; Chesneau, F.; Lucht, B.L. Surface phenomena of high energy  $\text{Li}(\text{Ni}_{1/3}\text{Co}_{1/3}\text{Mn}_{1/3})\text{O}_2$ /graphite cells at high temperature and high cutoff voltages. *J. Power Sources* **2014**, *269*, 920–926. [[CrossRef](#)]



© 2018 by the authors. Licensee MDPI, Basel, Switzerland. This article is an open access article distributed under the terms and conditions of the Creative Commons Attribution (CC BY) license (<http://creativecommons.org/licenses/by/4.0/>).